*International Journal of Automotive Technology*, Vol. 22, No. 4, pp. 979–992 (2021)
DOI 10.1007/s12239–021–0088–1

pISSN 1229–9138/ eISSN 1976–3832

# INTEGRATION OF ACTIVE TILTING CONTROL AND FULL-WHEEL STEERING CONTROL SYSTEM ON VEHICLE LATERAL PERFORMANCE

Wu Liang[1)], Ejaz Ahmad[2)], Muhammad Arshad Khan[2)] and Iljoong Youn[2)*]

[1)] State Key Laboratory of Automotive Simulation and Control, Jilin University, Changchun 130012, China
[2)]School of Mechanical, Aerospace & System Engineering, Gyeongsang National University, Jinju 52828, Korea

*(Received 24 June 2020; Revised 5 December 2020; Accepted 10 December 2020)*

**ABSTRACT**–This research presents an integration of two control systems, an active tilting controller and a full-wheel steering controller. This integration improves vehicle lateral performances by enhancing road-holding capability, lateral stability, and safety simultaneously. The active tilting controller utilizes an active mass shift to evenly distribute the vertical load at each suspension, and boost road-holding capability. On the other hand, the full-wheel steering controller adjusts rear steering angles to use lateral force at each ground-tyre contact point and amplify the vehicle's ability to follow the desired yaw rate and global sideslip angle during cornering maneuvers. Considering the improved road-holding capability and the coupling effect of body attitude motion and yaw motion, the two controllers in combination produce a synergistic effect on ride comfort, maneuverability and safety, and improve overall lateral performance. A 7-degree-of-freedom (DOF) linear full car model is used in designing the active tilting controller, while a 2-DOF bicycle model considering the attitude motion of the car body is used in designing a full-wheel steering controller. A 14-DOF complex nonlinear full car model that can truly reflect 6-DOF car body motion is applied to verify the performance of the proposed collaborative system. The simulation results show that the system represents a better lateral stability and steering response in intense driving while ensuring the better heading directivity of the vehicle.

**KEY WORDS** : Integrated control system, Active tilting control, Full-wheel steering control, Active rear steering, Preview control

NOMENCLATURE

| | | |
|---|---|---|
| $m$ | : vehicle sprung mass | kg |
| $J_x, J_y, J_z$ | : roll, pitch, yaw inertia | kg·m$^2$ |
| $g$ | : gravitational acceleration | m/s$^2$ |
| $a, b$ | : distance of c.g from right /left side | m |
| $c, d$ | : distance of c.g. from front and rear side | m |
| $h_r$ | : height from roll center to c.g. of car body | m |
| $l_f, l_r$ | : initial length of front and rear suspension | m |
| $l_{si}$ | : dynamic displacement of suspension | m |
| $k_i$ | : suspension spring stiffness | kN/m |
| $b_i$ | : suspension damping coefficient | N s/m |
| $\phi_n, \theta_n, \psi_n$ | : roll, pitch, and yaw angle of the car body | rad |
| $\omega_x, \omega_y, \omega_z$ | : roll, pitch and yaw angular velocity of car body | rad/s |
| $u, v, w$ | : longitudinal, lateral and vertical velocity of the car body | m/s |
| $F_{xgsi}, F_{ygsi}, F_{zgsi}$ | : longitudinal/ lateral/ vertical force at the tyre contact patch | N |
| $F_{xsi}, F_{ysi}, F_{zsi}$ | : longitudinal/ lateral/ vertical force acting at the mounting point of car body | N |
| $m_{ui}$ | : wheel mass | kg |
| $J_{wi}$ | : tyre rotational inertia | kg·m$^2$ |
| $k_{ti}$ | : tyre spring stiffness | kN/m |
| $C_{\lambda i}, C_{\alpha i}$ | : longitudinal, later stiffness | kN/rad |
| $r_{io}$ | : steady tyre radius | m |
| $r_i$ | : dynamic tyre radius | m |
| $\lambda_i$ | : longitudinal slip coefficient | |
| $\alpha_i$ | : sideslip angle of tyre | rad |
| $F_{xti}, F_{yti}$ | : longitudinal, lateral tyre force | n |
| $\omega_i$ | : tyre rotational angular velocity | rad/s |
| $\delta_i$ | : steering angle of the wheel | rad |

*Corresponding author. e-mail: iyoun@gnu.ac.kr

## 1. INTRODUCTION

In general, vehicle performance means to control its lateral, longitudinal, and vertical motions to enhance ride comfort, handling performance, and braking or traction performance. Electronic stability control (ESC), anti-lock braking system (Mirzaei and Mirzaeinejad, 2012; Topalov *et al.*, 2011), active front steering control (Zafeiropoulos and Di Cairano, 2013; Li *et al.*, 2014) and full-wheel steering control (Scherbring and Gust, 2013; Huashi, 2008) are the common examples to improve the vehicle performance. Each control system can be effective only within a specific region to achieve a particularly dynamic performance. For example (Farmer, 2004) an electronic stability controller is used to improve vehicle handling to prevent single-vehicle crashes. An ESC algorithm is presented (Zhai *et al.*, 2016) for four-wheel independent drive electric vehicles to improve vehicle stability during cornering.

These controllers might be able to influence the same vehicle dynamics or cause some coupling effect. Thus, the role of the integration of vehicle control is to coordinate the local components and handle the interactions between them. Since the performance specifications of local controllers are often in conflict, they must also guarantee a balance or trade-off between them(Gáspár *et al.*, 2016).

For enhancing vehicle lateral performance (road-holding capability, handling capability, lateral stability, and ride comfort), some control systems have been widely studied, as an active suspension system, anti-roll bar, active steering system, and braking distribution system. In (Attia *et al.*, 2019) an active suspension system within an identification technique is presented to estimate the vehicle dynamic model to improve ride comfort and vehicle handling capability in the presence of noise and center of gravity position uncertainties.

The advantage of active suspension is not just to reduce the impact of vertical road disturbance. It has the potential on vehicle lateral performance by tilting the car body to an expected attitude. A tilting system on rail and ground vehicles has been reported by (Goodall, 1999; Zhou *et al.*, 2011). The tilting angle was determined by the roll moment of the passive vehicle. In this way, the acceleration of passengers was reduced by about 30% (Wang and Shen, 2008). In (Zhou *et al.*, 2014), a robust estimation approach using $H_\infty$ algorithm is proposed to estimate the vehicle parameter variations. Here active lateral secondary suspension is integrated into the titling system to improve the trade-off between curving performance and straight track ride comfort. In (Saglam and Unlusoy, 2016), a state-dependent Riccati equation based control strategy is investigated to improve the ride comfort at low suspension deflection and to achieve proper attitude position at higher suspension deflection. (Cech, 2000) investigated an active roll and anti-roll control strategy to improve the cornering performance of the full car vehicle model. In a recently published paper (Ni *et al.*, 2020), posture control is represented.

Ride comfort in the lateral direction can be improved by an active tilting system (AST). However, it is not easy to reveal the relationship between active attitude changes and vehicle lateral stability. The yaw rate and roll angle of the vehicle are obviously affected by vertical force on the suspension. They are the main factors affecting the lateral stability of the vehicle(Esmailzadeh *et al.*, 2003; Esmailzadeh *et al.*, 2001; Song, 2005). In traditional ways to improve lateral stability, electronic stability control based on multiple brake control systems are currently used by many vehicles.

In (Tchamna *et al.*, 2014), ASI (active flat system which penalizes integration action of suspension deflection to keep body flat) was integrated with the ESC system to demonstrate an increase in lateral stability. (Čorić *et al.*, 2018) utilized active suspension control strategy to optimize the inputs which can reduce the braking distance and improve the vehicle stability performance. In (Smith *et al.*, 2018), an optimal controller-based torque vectoring (TV) controller is used to follow the reference yaw rate. The controller can compensate for the load transfer effects encountered during braking, acceleration, and high lateral acceleration.

The use of braking control will inevitably lead to unnecessary speed reduction. Recent research has shown that a four-wheel steering system including active rear steering (ARS) wheels can effectively improve the lateral stability of the vehicles without speed reduction, which set the rear wheels in the direction same to the front wheel steering angle at high speeds and improve vehicle handling by turning the rear wheels in the opposite direction of the front wheel angle at low speed. In (Lucet *et al.*, 2015), a path tracking controller is designed for a four-wheel steering vehicle to improve its performance on slippery surfaces. Here a cascaded sub-systems-based control strategy is used to first compute the tracking error for the lateral and heading deviations and then an adaptive predictive controller is applied to limit the wheel slippage and to prevent the vehicle from a harsh swing. In (Khan *et al.*, 2015) formulated a path-following control problem subjected to wheel slippage and skid and solves it using a logic-based control scheme for a wheeled mobile robot to control Longitudinal and lateral slip. (Li *et al.*, 2016) investigated the performance of the vehicle through the integration of direct yaw moment control and active steering control to follow the reference yaw rate and side-slip angle.

Replacing ESC with ARS can effectively improve lateral stability without sacrificing speed. In addition, AST is a necessary complement to the ARS system by evenly distributing the vertical dynamic load to enhance vehicle adhesion. This paper integrates an active tilting control with full-wheel steering control systems. The integration of two

controllers simultaneously enhance the road-holding capability,lateral stability, vehicle safety, vehicle handling and ride comfort, during cornering. Our previous work (Liang *et al.*, 2018; Wu *et al.*, 2016; Youn *et al.*, 2006; Youn *et al.*, 2015) has proved that when the vehicle turns, brakes and accelerates, the controller adjusts the body roll angle and the centre of gravity offset to 1) prevent the safety hazard caused by the lateral acceleration; 2) improves adhesion by the average vertical force distribution on tyres; 3) Improve the ride comfort by reducing the acceleration felt by the passenger. In (Ahmad *et al.*, 2020) we used a half car model equipped with active aerodynamic surfaces to improve ride comfort by reducing the sprungmass acceleration and road-holding capability by suppressing the vibrations in tyre deflection.

In this paper, the positive effect of AST in lateral stability and safety is emphatically investigated. The control gain of AST and ARS is derived by using optimal control theory, and the control gain is used in the collaborative controller of complex nonlinear active attitude variable vehicle model to make it more realistic and accurate. The vehicle's ride comfort, road-holding, lateral stability, handling and safety are effectively improved during cornering.

## 2. VEHICLE SYSTEM MODEL

In the previous work (Liang *et al.*, 2018), a nonlinear model of vehicle including an active passenger seat was derived to mainly describe acceleration response on passengers. In this paper, keeping the same parameter values, the active passenger seat is removed from the nonlinear vehicle model. The relationship between the Angular motion of the car body and handling performance is presented in detail. Figure 1 describes a complex mathematical model of a vehicle that accurately reflects the dynamic body attitude changes and their effects. It includes 6 degrees of freedom in the center of the body and 4 degrees of longitudinal and rotational freedom of the tyre. In order to design the active tilting controller, the complex model is simplified into a 7-DOF linear vehicle model that can reflect the attitude change and its response, and a 2-DOF bicycle model considering the effect of body tilting is used to design AST and ARS respectively. Complex nonlinear models can better represent the actual vehicle and better reflect the overall performance of the control system.

### 2.1. Active Tilting Control of Complex Non-linear Vehicle Model

The complex vehicle model mentioned in this paper describes the process of force transfer from the ground through the wheels and suspension to the vehicle body, which more accurately reflects the longitudinal, lateral, vertical, roll, pitch, and yaw motion of the body, as well as the vertical and rotational motion of the tyre.

As shown in Figure 2, the initial coordinate system

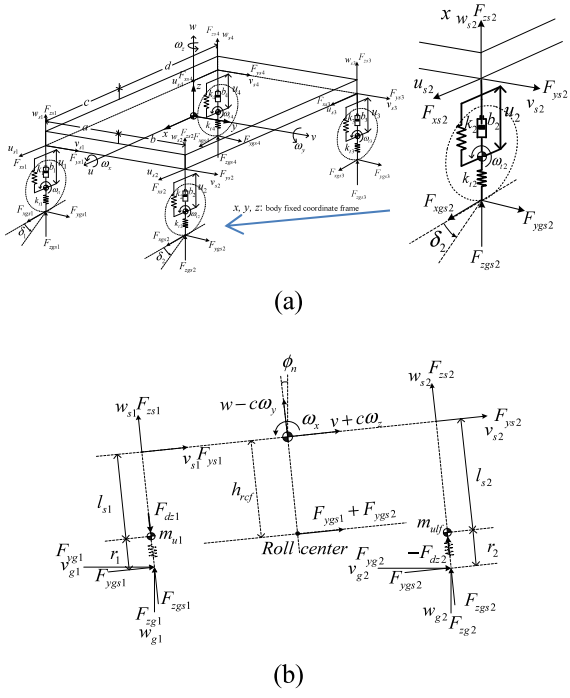


Figure 1. Complex nonlinear active attitude variable vehicle model.

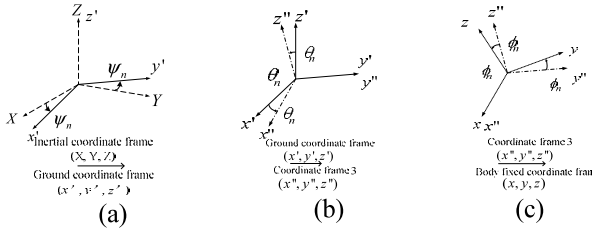


Figure 2. Coordinate transformation process from initial coordinate system to the fixed coordinate system of the vehicle body.

passes through the rotating yaw angle, Ψn, and obtains the ground coordinate system (x', y', z'). After rotating the pitch angle, θn, and then rotating the roll angle, φn, the fixed coordinate system (x, y, z) of the vehicle body is finally obtained. According to the above relationship, the conversion relationship from the ground coordinate system to the fixed coordinate system of the vehicle body can be obtained. The speed and force of the vehicle body relative to the fixed coordinate system of the vehicle body in Figure 1(a) can also be obtained by the above relationship.

Figure 3 describes the transformation process of velocities and forces from tyre-ground connected points to the car body at ith suspension mounting point. The source of all passive changes of positions and attitude of the car body is from various longitudinal and lateral friction forces

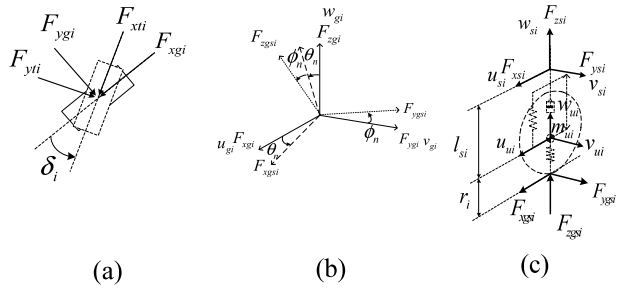

(a) (b) (c)

Figure 3. The force that the ground contact points transmit to the body.

$F_{xti}$ and $F_{yti}$ on the tyre-ground connected surface as shown in Figure 3(a). The friction forces can be transformed into the car body-fixed coordinate frame, as shown in Figure 3(b). Finally, all the position and attitude changes on the vehicle body caused by the friction forces and the vertical dynamic load are gradually transmitted to the vehicle body through the tyre and suspension system, as shown in Figure 3(c).

When the vehicle is turning, due to the inertia of the vehicle body and passive suspensions, the vehicle body is tilted towards the outside. Considering the roll center is located at the ground first, the total roll moment of the vehicle can be expressed as:

$$M_{xt} = \sum_{i=1}^{4} M_{xti} \tag{1}$$

where,

$$M_{xti} = F_{ygsi} r_i + F_{ysi} l_{si} \tag{2}$$

According to Figure 1(b), when the vehicle has a rolling center, the roll moment of the sprung mass can be calculated by the lateral force of the vehicle body and the distance from mass center to roll center as in (3).

$$M_{xi} = F_{ysi} h_r, i = 1 \sim 4 \tag{3}$$

The difference of total roll moment of vehicle and roll moment of sprung mass divided by wheelbase is lateral load transform which influences road-holding capability and lateral safety of the vehicle.

$$F_{dz1} = -F_{dz2} = \frac{M_{xt1} + M_{xt2} - (M_{x1} + M_{x2})}{(a+b)} \tag{4}$$

$$F_{dz4} = -F_{dz3} = \frac{M_{xt4} + M_{xt3} - (M_{x4} + M_{x3})}{(a+b)} \tag{5}$$

According to the above-mentioned force and velocity transformed from the ground coordinate system to the fixed coordinate system of the vehicle body, Newton's law, and Euler equation are used to derive the dynamic equation of the 6 DOF motion of the vehicle, as follows:

$$m(\dot{u} + \omega_y w - \omega_z v) = \sum_{i=1}^{4} F_{xsi} + mg \sin\theta_n \tag{6}$$

$$m(\dot{v} + \omega_z u - \omega_x w) = \sum_{i=1}^{4} F_{ysi} - mg \sin\phi_n \cos\theta_n \tag{7}$$

$$m(\dot{w} + \omega_x v - \omega_y u) = \sum_{i=1}^{4} (F_{zsi} + F_{dzi}) - mg \cos\phi_n \cos\theta_n \tag{8}$$

$$J_x \dot{\omega}_x = \sum_{i=1}^{4} M_{xi} - (F_{zs1} + F_{zs4})a + (F_{zs2} + F_{zs3})b \tag{9}$$

$$J_y \dot{\omega}_y = \sum_{i=1}^{4} M_{yi} - (F_{zs1} + F_{zs2})c + (F_{zs3} + F_{zs4})d \tag{10}$$

$$\begin{aligned} J_z \dot{\omega}_z &= (F_{xs1} + F_{xs4})a - (F_{xs2} + F_{xs3})b \\ &+ (F_{ys1} + F_{ys2})c - (F_{ys3} + F_{ys4})d \end{aligned} \tag{11}$$

The effects of vehicle lateral load transfer $F_{dzi}$ and mass shift, $mg \sin\phi_n \cos\phi_n$ are reflected in the vehicle lateral dynamics and vertical dynamics equations (7) and (8). It can be clearly seen from the above two equations that the influence of lateral load transfer, tyre dynamic load, and mass shift of the vehicle exacerbate the passive roll motion of the vehicle. For a conventional passive vehicle, lateral load transfer and passive mass shifting result in more serious body tilt, reduced steering sensitivity and grip, and even overturning. This further illustrates the importance of controlling the body attitude (especially for vehicles with a higher mass center). Finally, a vehicle model that can describe the influence of attitude change is obtained. By using Newton's law and Euler's equation, the dynamic equations with 25 system variables is presented. The system state vector, $x_n$, and disturbance vector, $w_n$ are represented as:

$$\begin{aligned} \mathbf{x_n} = [&u, v, w, \theta_n, \phi_n, \psi_n, \omega_y, \omega_x, \omega_z, \omega_{t1}, \omega_{t2}, \omega_{t3}, \omega_{t4}, \\ &d_{s1}, d_{s2}, d_{s3}, d_{s4}, d_{t1}, d_{t2}, d_{t3}, d_{t4}, w_{u1}, w_{u2}, w_{u3}, w_{u4}]^T \end{aligned} \tag{12}$$

$$\mathbf{W_n} = [w_{g1}, w_{g2}, w_{g3}, w_{g4}, \beta_1, \beta_2, \tau_b]^T \tag{13}$$

2.2. Simplified 7-DOF Full Car Model

In order to design the active tilting controller (AST), the model needs to be further simplified. A simplified 7-DOF linear model, such as in Figure 4, includes roll, pitch, and

vertical motion of car body as well as vertical motion of the four wheels while keeping the effect of passive and active mass shifting of the car body. The dynamic equations are as follows:

$$m\,\ddot{z}_c = \sum_{i=1}^{4} f_i \tag{14}$$

$$J_x\ddot{\phi}_l = \sum_{i=1}^{4} M_{xi} - (f_1 + f_4)a + (f_2 + f_3)b \tag{15}$$

$$J_y\ddot{\theta}_l = \sum_{i=1}^{4} M_{yi} - (f_1 + f_2)c + (f_3 + f_4)d \tag{16}$$

$$m_{ui}\ddot{z}_{ui} = k_{ti}(z_{oi} - z_{ui}) - f_i \tag{17}$$

where $i$ denotes the number of suspensions connected to the body, the roll and pitch moment of the car body, are taken directly from the complex model. The resultant force of the suspension system is generated by springs, dampers, and actively controlled actuators.

$$\begin{aligned} f_1 &= k_1(z_{u1} - z_c + c\theta_l + a\phi_l) \\ &+ b_1(\dot{z}_{u1} - \dot{z}_c + c\dot{\theta}_l + a\dot{\phi}_l) + u_1 \end{aligned} \tag{18}$$

$$\begin{aligned} f_2 &= k_2(z_{u2} - z_c + c\theta_l - b\phi_l) \\ &+ b_2(\dot{z}_{u2} - \dot{z}_c + c\dot{\theta}_l - b\dot{\phi}_l) + u_2 \end{aligned} \tag{19}$$

$$\begin{aligned} f_3 &= k_3(z_{u3} - z_c - d\theta_l - b\phi_l) \\ &+ b_3(\dot{z}_{u3} - \dot{z}_c - d\dot{\theta}_l - b\dot{\phi}_l) + u_3 \end{aligned} \tag{20}$$

$$\begin{aligned} f_4 &= k_4(z_{u4} - z_c - d\theta_l + a\phi_l) \\ &+ b_4(\dot{z}_{u4} - \dot{z}_c - d\dot{\theta}_l + a\dot{\phi}_l) + u_4 \end{aligned} \tag{21}$$

According to the above equations, a 7-DOF vehicle model considering the influence of roll and pitch moments is established. The system state and disturbance vector of the model are defined as follows:

$$\begin{aligned} \boldsymbol{x} = [&\dot{z}_c, \theta_l, \phi_l, \dot{\theta}_l, \dot{\phi}_l, z_{u1} - z_c + c\theta_l + a\phi_l, \\ &z_{u2} - z_c + c\theta_l - b\phi_l, z_{u3} - z_c - d\theta_l - b\phi_l, \\ &z_{u4} - z_c - d\theta_l + a\phi_l, z_{o1} - z_{u1}, z_{o2} - z_{u2}, \\ &z_{o3} - z_{u3}, z_{o4} - z_{u4}, \dot{z}_{u1}, \dot{z}_{u2}, \dot{z}_{u3}, \dot{z}_{u4}]^T \end{aligned} \tag{22}$$

$$\boldsymbol{w} = [\dot{z}_{01}, \dot{z}_{02}, \dot{z}_{03}, \dot{z}_{04}, M_x, M_y]^T \tag{23}$$

### 2.3. Simplified Lateral Control Bicycle Model

In order to verify the positive influence of active tilting control on vehicle lateral performance, this paper designs the vehicle lateral stability and trajectory tracking controller by using the 2-DOF bicycle model to analyze the vehicle

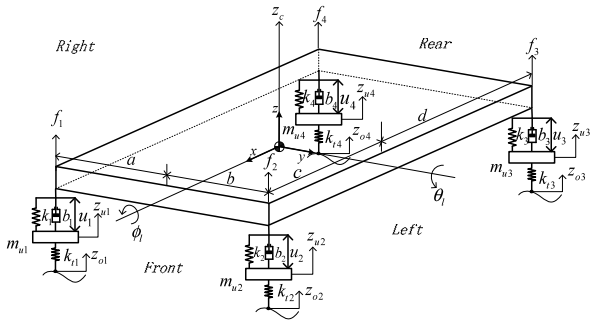


Figure 4. Linear simplified model considering the influence of attitude changes.

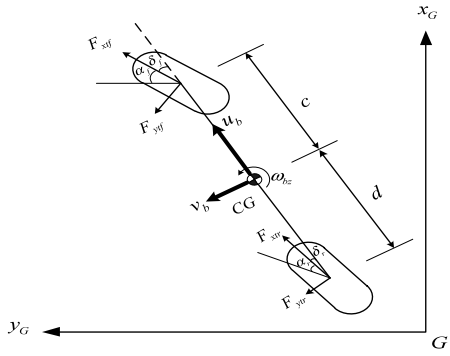


Figure 5. Linear simplified model considering the influence of attitude changes.

lateral performance. Assume that the vehicle is traveling on a horizontal road. The rolling angle of the car body can be given by a complex passive system or active system, which is used to compare the effect of variations in active body motion. The vertical and pitch motions of the sprung mass and all motions of the unsprung mass are ignored, only the yaw and lateral motion of the sprung mass are considered, as shown in Figure 5. $F_{xtf}$ and $F_{ytf}$ are longitudinal and lateral tyre forces.

This paper assumes that the vehicle is running at a high speed and has a small steering angle, so the longitudinal dynamic equation can be omitted. This 2-DOF bicycle model including yaw and lateral motion is expressed as:

$$m(\dot{v}_b + u_b\omega_{bz}) = 2F_{ytf} + 2F_{ytr} - mg\sin\theta_r \tag{24}$$

$$J_z\dot{\omega}_{bz} = 2cF_{ytf} - 2dF_{ytr} \tag{25}$$

$$F_{ytf} = -C_{\alpha f}\alpha_{fs} \tag{26}$$

$$F_{ytr} = -C_{\alpha r}\alpha_{rs} \tag{27}$$

$u_b$ represents the longitudinal speed of the vehicle, $C_{af}$ and $C_{ar}$ refers to the lateral stiffness of the front and rear wheels. The side-slip angles of the front and rear wheels are expressed as:

$$\alpha_{fs} = \frac{v_b + c\omega_{bz}}{u_b} - \delta_f \tag{28}$$

$$\alpha_{rs} = \frac{v_b - d\omega_{bz}}{u_b} - \delta_r \tag{29}$$

In the case of stable control, the front wheel steering angle is given by the driver and can be used as an external disturbance to the system. The rear-wheel steering angle is the controller input that reduces the error between the ideal vehicle control target and the actual system output.

The equation for the bicycle model can be modified to the system state equation (30). The lateral velocity $v_b$ and yaw rate $w_{bz}$ are two system state variables $x_{b1}$ and $x_{b2}$. The front steering angle $\delta_f$ is the external disturbance given by the driver. The rear steering angle $\delta_r$, is the control input obtained by minimizing the difference between the ideal and actual yaw rate and global sideslip angle of the vehicle.

$$\begin{aligned}&\mathbf{x}_b(k+1) = \\ &\mathbf{A}_{b1}\mathbf{x}_b(k+1) + \mathbf{B}_{b1}\mathbf{u}_b(k) + \mathbf{D}_{b1}\mathbf{w}_b(k)\end{aligned} \tag{30}$$

Where

$$\boldsymbol{A_{b1}} = \boldsymbol{I} + \boldsymbol{A_b}\Delta t, \boldsymbol{B_{b1}} = \boldsymbol{B_b}\Delta t, \boldsymbol{D_{b1}} = \boldsymbol{D_b}\Delta t$$

$$\boldsymbol{A_b} = \begin{bmatrix} -2\dfrac{C_{\alpha f} + C_{\alpha r}}{mu_b} & -u_b - 2\dfrac{cC_{\alpha f} - dC_{\alpha r}}{mu_b} \\ -2\dfrac{cC_{\alpha f} - dC_{\alpha r}}{J_z u_b} & -2\dfrac{c^2 C_{\alpha f} + d^2 C_{\alpha r}}{J_z u_b} \end{bmatrix} \tag{31}$$

$$\boldsymbol{B_b} = \begin{bmatrix} 2\dfrac{C_{\alpha r}}{m} \\ 2\dfrac{-dC_{\alpha r}}{J_z} \end{bmatrix} \tag{32}$$

$$\boldsymbol{D_b} = \begin{bmatrix} 2\dfrac{C_{\alpha f}}{m} \\ 2\dfrac{cC_{\alpha f}}{J_z} \end{bmatrix} \tag{33}$$

2.4. Ideal Yaw Rate and Global Sideslip Angle of Vehicle

By using an active or semi-active suspension system, body undulations and sway can be significantly reduced. However, during cornering the lateral accelerations can still cause the passenger to feel uncomfortable and results in excessive changes in the dynamic tyre load. In order to further balance the effects of lateral acceleration which is parallel to the vehicle plane, the body needs to be inclined at an angle opposite to the direction of the centrifugal force. Figure 6 shows that the car body can achieve an ideal roll angle to overcome the centrifugal forces, as follows:

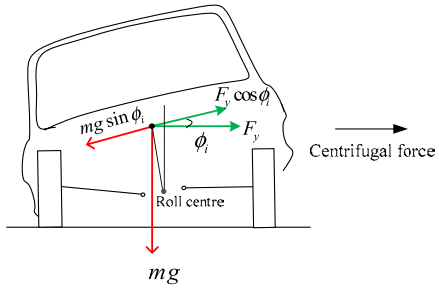


Figure 6. Optimal active attitude angle of the body.

$$\begin{aligned} &mg\ sin\ \phi_i = F_y\ cos\ \phi_i, \\ &F_y = ma_{cr} \Rightarrow \frac{a_{cr}}{g} = tan\ \phi_i \\ &\phi_i = arctan(\frac{a_{cr}}{g}) \end{aligned} \tag{34}$$

In equation (34), $\phi_i$ and $a_{cr}$ represent the desired roll angle and lateral acceleration during cornering, $F_y$ is a lateral force acting on the mass centre of the car body. AST system will tilt the body to the desired angle, which can minimize the lateral acceleration to improve the ride comfort. At the same time, the excessive dynamic tyre load caused by the external acceleration tends to be balanced, because the active component of gravity $mg\ cos\ \phi_n\ cos\ \theta_n$ neutralizes lateral load transfor $\sum_{i=1}^{4} F_{dzi}$ in equation (8). Based on the relationship between the cornering stiffness and vertical dynamic tyre load, it can be seen that the combined friction forces of left and right tyres are further enhanced when the vehicle is turning. Vehicle yaw rate and global sideslip angle are two key factors for lateral stability and safety performance. The yaw rate can be used to determine the three steering behavior states: over-steering, under-steering, and neutral-steering. Neutral-steering describes the actual steering maneuver is consistent with the state envisioned by the driver, or the vehicle traveling at the desired yaw rate and global side slip angle.

$$\omega_{zd} = \frac{u_b}{R} = \frac{u_b}{(c+d)} \cdot \delta_f \tag{35}$$

$$\beta_d = \frac{d - \frac{cmv_b^2}{2C_{\alpha r}(c+d)}}{(c+d) + \frac{mv_b^2(dC_{\alpha r} - cC_{\alpha f})}{2C_{\alpha f}C_{\alpha r}(c+d)}} \cdot \delta_f \tag{36}$$

The vehicle steering characteristics may be determined by the actual yaw rate if is greater than or less than the desired yaw rate. Equation (35) is used to determine the desired yaw rate. Minimizing the error of the actual and desired yaw rate of the vehicle may make it easier to achieve neutral steering. Since it is safer for a high-speed vehicle to have a tendency to under-steer from a safety perspective, the controller is designed to be more biased towards a slight under-steer. The global sideslip angle (36) refers to the angle between the longitudinal axis of the vehicle body and the actual direction in which the vehicle is traveling. The desired vehicle global side slip angle is calculated based on the inherent steering characteristics of the vehicle and the grip condition.

## 3. CONTROLLER DESIGN FOR ATTITUDE AND LATERAL CONTROL OF VEHICLE

In this part, the optimal state tracking controllers of AST and ARS systems are designed by using the optimal control method respectively. The system performance is tested by comparing the body roll angle, $\phi_d$, the error between the ideal and actual values of $w_{zd}$ and global sideslip angle $\beta$. The linear models are derived from the discrete-time state-space matrix equations. Finally, optimal control gains obtained from linear models are applied to the composite nonlinear model corresponding to the same system states in linear and nonlinear models. By using the fourth-order Runge-Kutta algorithm, the nonlinear differential equation is solved as follows.

$$\boldsymbol{x_n}(k+1) = \boldsymbol{x_n}(k) + \frac{\Delta t}{6}(\boldsymbol{k_1} + 2\boldsymbol{k_2} + 2\boldsymbol{k_3} + \boldsymbol{k_4}) \tag{37}$$

### 3.1. Optimal Attitude Controller Design

First, based on the 7-DOF vehicle model, an active tilting controller (AST) is designed. System state and disturbance vector of the model is given as follows:

$$\begin{aligned}\boldsymbol{x} = [&\dot{z}_c, \theta_l, \phi_l, \dot{\theta}_l, \dot{\phi}_l, z_{u1} - z_c + c\theta_l + a\phi_l,\\ &z_{u2} - z_c + c\theta_l - b\phi_l, z_{u3} - z_c - d\theta_l - b\phi_l,\\ &z_{u4} - z_c - d\theta_l + a\phi_l, z_{o1} - z_{u1}, z_{o2} - z_{u2},\\ &z_{o3} - z_{u3}, z_{o4} - z_{u4}, \dot{z}_{u1}, \dot{z}_{u2}, \dot{z}_{u3}, \dot{z}_{u4}]^T\end{aligned} \tag{38}$$

$$\boldsymbol{w} = [\dot{z}_{01}, \dot{z}_{02}, \dot{z}_{03}, \dot{z}_{04}, M_x, M_y]^T \tag{39}$$

The performance index, (40) is minimized with 16 weighting factors. These indicators include heaving acceleration $\dot{x}_1$, roll and pitch acceleration $\dot{x}_{4\sim5}$, suspension deflection $x_{6\sim9}$, expected and actual body roll angle error $x_{d3} - x_3$, tyre deflection $x_{10\sim13}$, and vertical control forces $u_{1\sim4}$ provided by the four active actuators.

$$\begin{aligned}J = \lim_{T\to\infty}\frac{1}{2T}\int_0^T \{&\rho_1\dot{x}_1^2 + \rho_2\dot{x}_4^2 + \rho_3\dot{x}_5^2 + \rho_4 x_6^2 + \rho_5 x_7^2\\ &+\rho_6 x_8^2 + \rho_7 x_9^2 + \rho_8(x_{d3} - x_3)^2 + \rho_9 x_{10}^2 + \rho_{10} x_{11}^2\\ &+\rho_{11} x_{12}^2 + \rho_{12} x_{13}^2 + \rho_{13} u_1^2 + \rho_{14} u_2^2 + \rho_{15} u_3^2 + \rho_{16} u_4^2\}dt\end{aligned} \tag{40}$$

The performance index for the discrete-time control algorithm can be modified as quadratic forms of errors of desired states with system state, disturbance, and control forces. By minimizing $J$, the optimal tracking control force can be obtained through a series of calculations, as follows:

$$\begin{aligned}\mathbf{u}(k) = &-(\mathbf{R} + \mathbf{B}_1^T\mathbf{P}\mathbf{B}_1)^{-1}\cdot\{(\mathbf{B}_1^T\mathbf{P}\mathbf{A}_1 - \mathbf{N}_1^T)\mathbf{x}(k)\\ &+(\mathbf{M}_1^T + \mathbf{B}_1^T\mathbf{P}\mathbf{D}_1)\mathbf{w}(k) + \mathbf{N}_1^T\mathbf{x}_d(k) + \mathbf{B}_1^T\mathbf{b}_R^T(k+1)\}\end{aligned} \tag{41}$$

Finally, substituting the optimal tracking control force (41) into the linear state space equation, the closed loop system equation of the 7-DOF linear full car model can be written by

$$\begin{aligned}\mathbf{x}(k+1) = &\left(\mathbf{A}_1 - \mathbf{B}_1(\mathbf{R} + \mathbf{B}_1^T\mathbf{P}\mathbf{B}_1)^{-1}(\mathbf{B}_1^T\mathbf{P}\mathbf{A}_1 - \mathbf{N}_1^T)\right)\mathbf{x}(k)\\ &+\left(\mathbf{D}_1 - \mathbf{B}_1(\mathbf{R} + \mathbf{B}_1^T\mathbf{P}\mathbf{B}_1)^{-1}(\mathbf{M}_1^T + \mathbf{B}_1^T\mathbf{P}\mathbf{D}_1)\right)\mathbf{w}(k)\\ &-\mathbf{B}_1(\mathbf{R} + \mathbf{B}_1^T\mathbf{P}\mathbf{B}_1)^{-1}\mathbf{N}_1^T\mathbf{x}_d(k) - \mathbf{B}_1(\mathbf{R} + \mathbf{B}_1^T\mathbf{P}\mathbf{B}_1)^{-1}\mathbf{B}_1^T\mathbf{b}_R^T(k+1)\end{aligned} \tag{42}$$

### 3.2. Lateral Controller Design

For the active steering controller (ARS) design, the performance index $J_b$ is constrained by the same principle as described above. The performance index includes four weighting factors, which are yaw angular acceleration $\dot{x}_{b2}$, expected and actual yaw angular velocity error $x_{b2} - x_{bd2}$, controlled rear-wheel steering angle $u_b$, and the global side slip angle $\beta$. When designing a lateral stability controller, it is considered that the reduction of the global side slip angle is an important criterion of vehicle safety in cornering. If the global side slip angle of the vehicle is smaller than the acceptable side slip angle (36), it means lateral safety of the vehicle is enhanced. Therefore, the actual value of the yaw angle should be close to the ideal yaw rate, while ensuring a smaller global side slip angle. It should be noted that in the case of 2-DOF bicycle model, there is no variable directly giving the global side slip angle, $\beta$. Because of $\beta = tan^{-1}(\frac{V_b}{u_b})$, $V_b$ is penalized instead of $\beta$ in performance index.

$$J_b = \lim_{T\to\infty}\frac{1}{2T} \tag{43}$$

$$\int_0^T \{\rho_{b1}\dot{x}_{b2}{}^2 + \rho_{b2}(x_{b2} - x_{bd2})^2 + \rho_{b3}u_b{}^2 + \rho_{b4}x_{b1}{}^2\}\mathrm{d}t$$

In the same manner, the optimal control force for the 2-DOF bicycle model can be obtained by

$$\begin{aligned}\mathbf{u}_b(k) = &-(\mathbf{R}_b + \mathbf{B}_{b1}^{\mathrm{T}}\mathbf{P}_b\mathbf{B}_{b1})^{-1}\cdot \\ &\{(\mathbf{B}_{b1}^{\mathrm{T}}\mathbf{P}_b\mathbf{A}_{b1} - \mathbf{N}_{b1}^{\mathrm{T}})\mathbf{x}_b(k) + (\mathbf{M}_{b1}^{\mathrm{T}} + \mathbf{B}_{b1}^{\mathrm{T}}\mathbf{P}_b\mathbf{D}_{b1})\mathbf{w}_b(k) \\ &+\mathbf{N}_1^{\mathrm{T}}\mathbf{x}_{db}(k) + \mathbf{B}_{b1}^{\mathrm{T}}\mathbf{b}_{Rb}^{\mathrm{T}}(k+1)\}\end{aligned} \tag{44}$$

The feed-forward control gain $\mathbf{b}_{Rb}(k)$, $k = (t/\Delta t)\sim(t_p/\Delta t - 1)$ can be calculated as follows.

$$\begin{aligned}\mathbf{b}_{Rb}(k) = &-\mathbf{x}_{db}^{\mathrm{T}}(k)(\mathbf{Q}_b + \mathbf{N}_1(\mathbf{R}_b + \mathbf{B}_{b1}^{\mathrm{T}}\mathbf{P}_b\mathbf{B}_{b1})^{-1}(\mathbf{B}_{b1}^{\mathrm{T}}\mathbf{P}_b\mathbf{A}_{b1} - \mathbf{N}_{b1}^{\mathrm{T}})) \\ &-\mathbf{w}_b^{\mathrm{T}}(k)((\mathbf{M}_{b1} + \mathbf{D}_{b1}^{\mathrm{T}}\mathbf{P}_b\mathbf{B}_{b1})(\mathbf{R}_b + \mathbf{B}_{b1}^{\mathrm{T}}\mathbf{P}_b\mathbf{B}_{b1})^{-1}(\mathbf{B}_{b1}^{\mathrm{T}}\mathbf{P}_b\mathbf{A}_{b1} - \mathbf{N}_{b1}^{\mathrm{T}}) \\ &-(\mathbf{D}_{b1}^{\mathrm{T}}\mathbf{P}_b\mathbf{A}_{b1} - \mathbf{N}_{12}^{\mathrm{T}})) + \mathbf{b}_{Rb}(k+1)(\mathbf{A}_{b1} \\ &-\mathbf{B}_{b1}(\mathbf{R}_b + \mathbf{B}_{b1}^{\mathrm{T}}\mathbf{P}_b\mathbf{B}_{b1})^{-1}(\mathbf{B}_{b1}^{\mathrm{T}}\mathbf{P}_b\mathbf{A}_{b1} - \mathbf{N}_{b1}^{\mathrm{T}}))\end{aligned} \tag{45}$$

## 4. SIMULATION ANALYSIS

When the vehicle is traveling in cornering, the lateral acceleration and steering characteristics of the vehicle not only affect the ride comfort but more importantly, it influence the lateral stability, the safety of the vehicle. Four different systems are illustrated in this simulation part, as the vehicle with passive suspension (PS), the vehicle with attitude flat control (ASI), the vehicle with active tilting control (AST), the vehicle with full-wheel steering control (ARS), and vehicle with the proposed cooperative control (AST & ARS).

In general, the size of the vehicle is symmetrical in all directions, so the mass center is considered to coincide with the geometric center of the vehicle. The potential of tilting controller on vehicle road-holding capability in cornering is investigated through MATLAB software simulation in section 4.1. Then the performance between the proposed collaborative system and independent control system is analyzed.

The values of weighting factors in Table 1 are determined by considering ride comfort, handling, and attitude motion. The weighting parameters of the AST system ensures the minimum error between the ideal attitude angle and the actual angle, and improve the ride comfort and road-holding capability. The weighting parameters of the ARS system ensures the minimum error of ideal and actual yaw rate and enhance lateral safety.

To calculate the feedforward parts $b_R$, the desired roll angle $x_d$, must be predicted from present to 0.3 seconds ahead for each sampling time, because the 0.3 seconds preview time is suitable to get full advantage of preview information.

Table 1. Performance parameter weight values.

| | Target | Weights |
|---|---|---|
| AST | Vehicle acceleration | $\rho_1 = 1$ |
| | Pitch and roll acceleration | $\rho_{2,3} = 1$ |
| | Suspension relative displacement | $\rho_{4,5,6,7} = 1$ |
| | Ideal and actual body tilt angle error | $\rho_8 = 10^5$ |
| | Relative displacement of tyre | $\rho_{9,10,11,12} = 10^4$ |
| | Attitude control unit | $\rho_{13,14,15,16} = 10^{-5}$ |
| ARS | Yaw angle acceleration | $\rho_{b1} = 1$ |
| | Ideal and real angular velocity error | $\rho_{b2} = 10000$ |
| | Rear wheel angle | $\rho_{b2} = 0.0001$ |
| | Side-slip angle | $\rho_{b3} = 100$ |

### 4.1. Case 1 J-turn Maneuver

First, the vehicle traveling at 80 km/h on a dry asphalt road. A J-turn maneuver is used to test the control performance in a steady steering curve condition. It is assumed that the center of mass the vehicle plays a vital role in vehicle steering characteristics. If the vehicle's mass center is closer to the front wheel, the vehicle behaves as under-steering. Similarly, if the mass center is closer to the rear wheels, the vehicle behaves as an over-steering. In this case, the mass center of the car body is located at the geometric center of the car body (c=d), then this vehicle presents neutral-steer behavior. Three systems ASI, AST, and PS are compared for investigation of attitude control as follows. Figures 7 and 8 represent a front-wheel steer input and the generated centrifugal force on the mass center. According to the centrifugal force, the desired roll angle of the car body is computed by Equation (34).

In Figure 9, due to the centrifugal force, the passive system (PS) is tilted approximately 1.8 degrees outward. Comparing with PS, ASI which has been done in the previous research can reduce the roll angle of the car body and keeps the roll angle close to 0 degrees. The active tilting control system (AST) mentioned in this paper can make the body tilt actively towards inside when turning, and the actual output value of the system can track the desired trajectory of the ideal roll angle. Since the controller design has considered the suspension, the tyre, and the interference generated by the inertial force of the vehicle during the attitude adjustment process, it can be seen that the angular error of AST is minimized to meet the design requirements. AST is an active tilting system based on a simplified 7-DOF linear full car model, which is applied

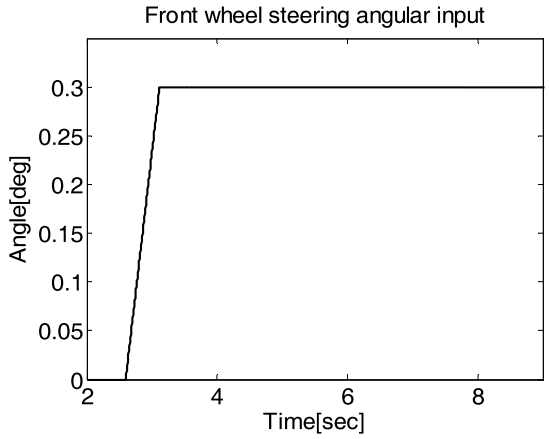


Figure 7. Front wheel steering input.

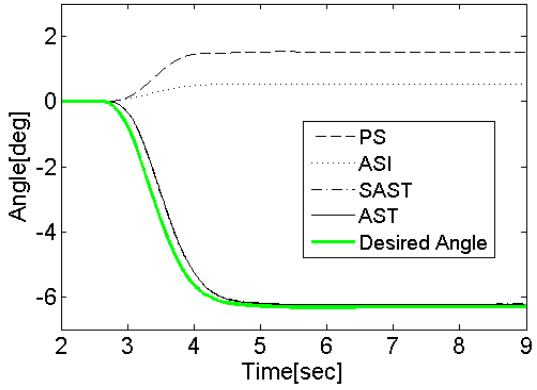


Figure 9. Changes in body angle of several systems mentioned.

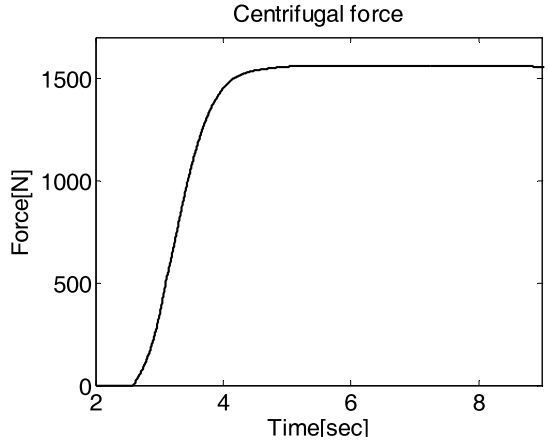


Figure 8. Centrifugal force on the body.

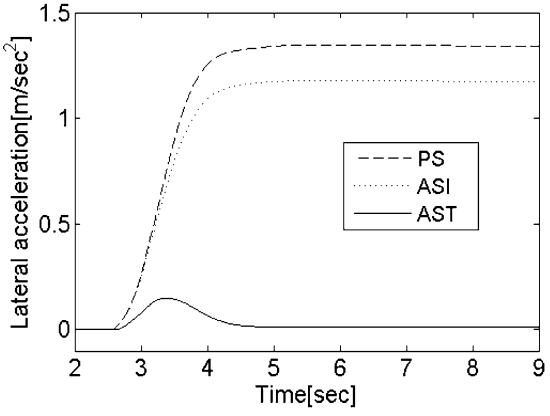


Figure 10. Acceleration of passengers.

to nonlinear 14-DOF complex model. The results of the linear model SAST and nonlinear model AST are very close. The tilting controller which is designed based on the linear model is also effective in the nonlinear model. Figure 10 shows the lateral acceleration variations, which are parallel to the plane of the body. It can be clearly seen that PS has the largest lateral acceleration (1.35 $ms^{-2}$) as compared to lateral acceleration of ASI (1.1 $ms^{-2}$) This is because ASI only can prevent the car body from leaning outward and reduce the impact of mass shift, the unpleasant lateral acceleration is still acting on passengers. AST can use the active mass shift of the car body to balance most of the lateral acceleration effects, which greatly improves the ride comfort during cornering.

The advantage of AST is not only to balance out the uncomfortable acceleration on passengers but also to evenly distribute the vertical dynamic load on both sides of the vehicle in cornering. Figure 11 shows the tyre deflection of the two front wheels in the PS, AST, and ASI systems. The tyre deflection for PS is 0.0213 m for ASI is 0.0212 m and for AST the tyre deflection is 0.012. Hence it is obvious that AST can effectively balance tyre deflections of left and right wheels and improve road-holding capability in cornering. Figure 12 shows the lateral friction forces of two front wheels calculated from the amount of tyre deflection, friction coefficient, and the inherent characteristics of the tyre. As shown in Figure 12, unlike other systems, both sides of lateral friction forces of AST are almost equal. That is to say, the mass shifting caused by active tilting balances out the roll moment generated by centrifugal forces. Another key issue is that the evenly distributed tyre force also enhances the effectiveness of ARS, thereby contributing to the synergy of the proposed collaborative controller.

Hence proved that ARS is an effective method for lateral stability control. This part will further illustrate the interaction of AST and ARS in lateral stability by the given J turn maneuver. As shown in Figures 13 and 14, when the vehicle is set to neutral-steering behavior, the yaw rate and global sideslip angle of all systems (PS, ASI, and AST) satisfy the desired values $2.6\,deg\,s^{-1}$ at a steady state.

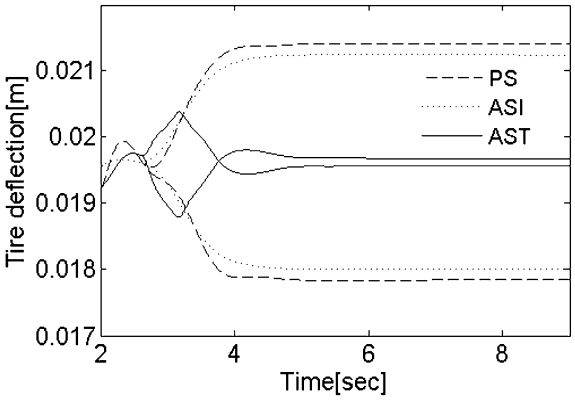


Figure 11. Tyre deformation of the two front wheels of different systems.

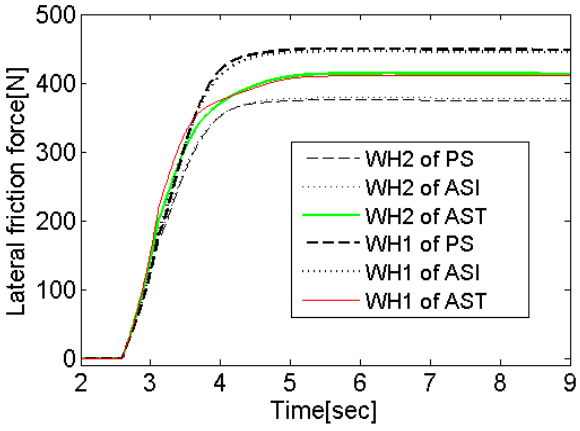


Figure 12. Lateral friction of the two front wheels of different systems.

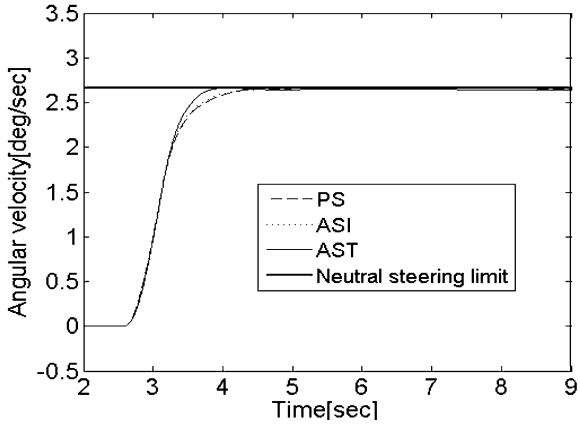


Figure 13. Yaw rate of the vehicle with neutral-steering behavior.

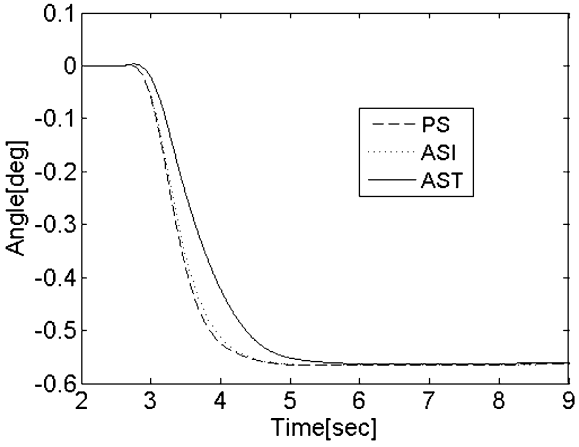


Figure 14. Global sideslip angle of the vehicle with neutral-steering behavior.

However, AST shows the simultaneous improvement of the transient response for yaw rate and reduction for global sideslip angle. The reduction of global side slip angle and yaw rate response time indicates that the AST can enhance vehicle steering sensitivity while enhancing the lateral safety in cornering.

Now, it is assumed that the mass center of the vehicle moves toward the rear side of the vehicle (c = 1.35 m, d = 1.15 m). When the vehicle is turned at a high speed, it exhibits over-steering behavior, which will have a negative impact on lateral stability and safety. As shown in Figure 15, the vehicle exhibits over-steering behavior. Without the intervention of ARS, AST is not sufficient to change the steering characteristics of the vehicle. ARS can directly control the rear steer angle to track the ideal yaw rate without using any braking force. In Figure 16, AST can reduce global sideslip angle (-0.3 deg) to make the vehicle safety, as compared to PS (-1 deg), ARS (-0.7 deg), but still exceeds the reasonable global sideslip angle calculated by equation (36). It shows that when the vehicle has over-steering characteristics, AST worked independently, and cannot meet the vehicle's lateral safety objective. Therefore, ARS must be worked in conjunction with AST to effectively control the yaw rate and global sideslip angle. When ARS is in operation, both PS & ARS and AST & ARS can produce expected results. The actual yaw rate is reduced and a slight under-steering behavior is maintained. However, when the yaw rate of the two systems remains relatively closed, the global sideslip angle of AST & ARS can be significantly reduced. This result indicates the potential of the collaborative system for the improvement of lateral stability and safety.

Next, the effectiveness of the coordinated control system under different operating conditions is tested by inputting other steering commands to front wheels.

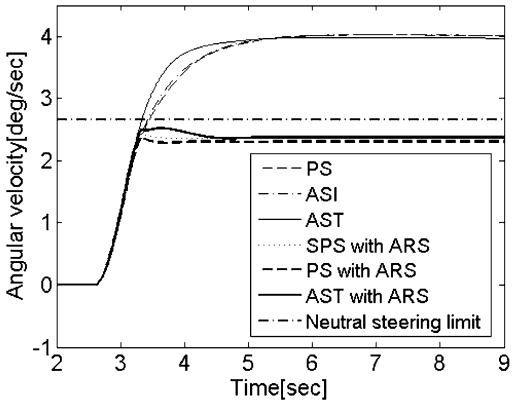


Figure 15. Yaw rate of the vehicle with over-steering behavior.

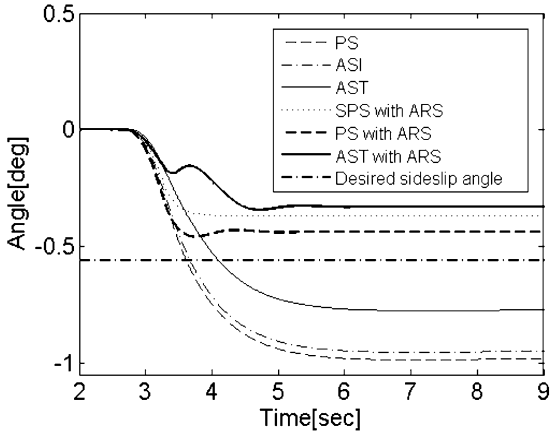


Figure 16. Global sideslip angle of the vehicle with over-steering behavior.

4.2. Case 2. Fishhook Maneuver

Fishhook maneuver is usually utilized to test the vehicle for avoiding rollover under extreme conditions. Car speed and road conditions are the same as in case 1. Figure 17 shows the centrifugal force produced by the given fishhook front-wheel steering angle when the vehicle has neutral-steering or over-steering behavior.

The lateral safety is very much important in this case. Tyre deflections of the left and right front wheels of the vehicle with different steering behavior are represented in Figures 18 and 19. Because tyre deflection is directly related to dynamic vertical load on four wheels, the results show AST can evenly balance the vertical dynamic load on the left and right sides of the vehicle with two kinds of steering behavior. This means the proposed AST has the ability to avoid rollover, no matter what steering behavior the vehicle has.

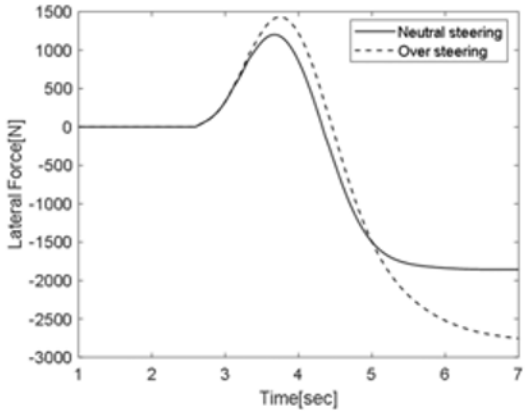


Figure 17. Centrifugal force with different steering characteristics.

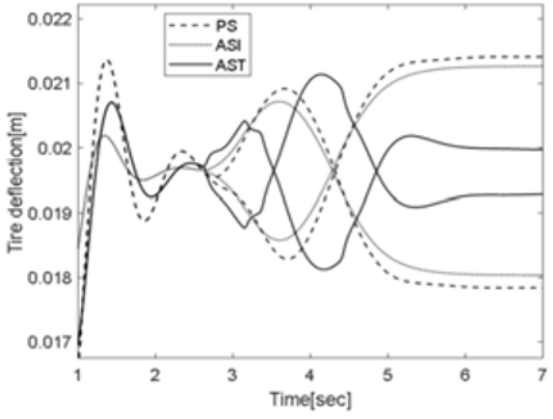


Figure 18. Tyre deflection of the vehicle with neutral steering.

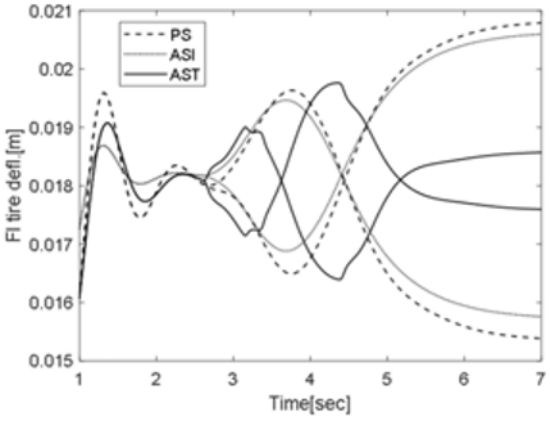


Figure 19. Tyre deflection of the vehicle with over-steering.

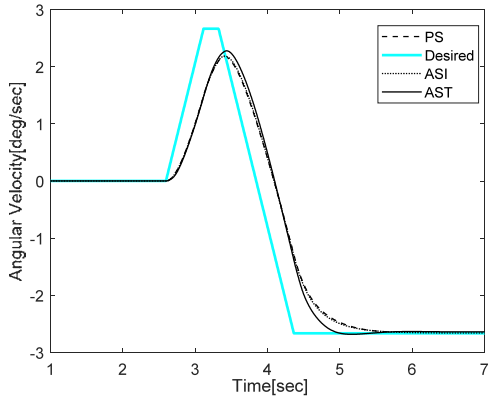


Figure 20. Yaw rate of vehicle with neutral steering behavior.

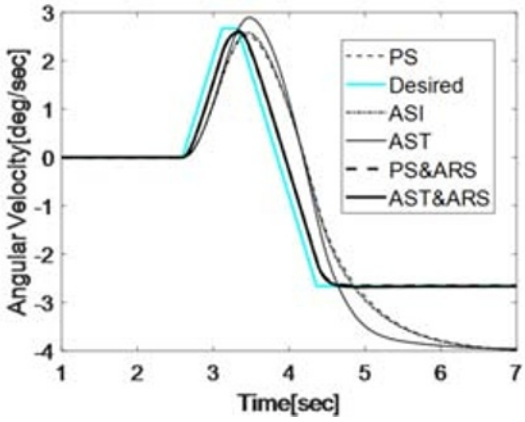


Figure 22. Yaw rate of vehicle with over-steering behavior.

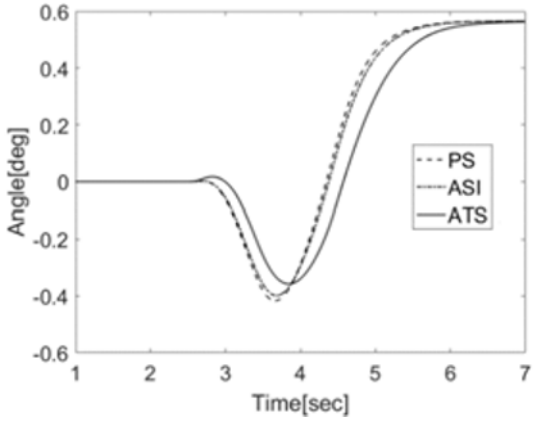


Figure 21. Global sideslip angle of vehicle with neutral steering behavior.

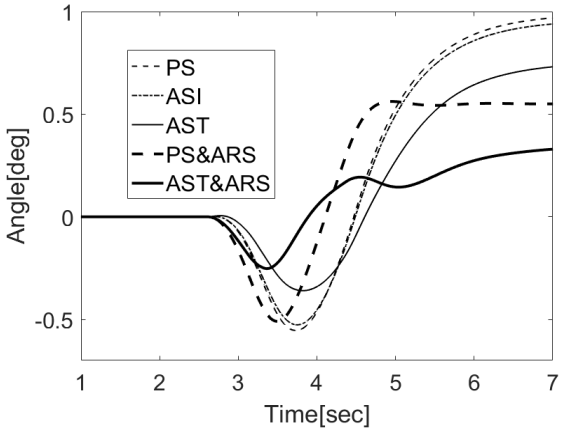


Figure 23. Global sideslip angle of the vehicle with over-steer behavior.

The criterion of lateral stability and safety is related to yaw rate and global sideslip angle. As shown in Figures 20 and 21, yaw rate and global side slip angle of the vehicle with neutral steering behavior is described. All systems are satisfied the criterion of lateral stability and safety according to equations (35) and (36), however, AST presents a simultaneous faster response on yaw rate and a reduction on global sideslip angle of the vehicle.

As shown in Figures 22 and 23, when the vehicle exhibits over-steering behavior, AST is not sufficient to change the steering characteristics of this vehicle without the intervention of ARS. ARS can directly control the rear steer angle to track the ideal yaw rate without using any braking forces and reduce the global sideslip angle to avoid a dangerous behavior of the vehicle. However, AST & ARS in Figure 23 describes an obvious reduction on global sideslip angle compared to PS & ARS. The decreased trend of global sideslip angle is similar to the result given in Figure 16. The result of the collaborative system shows an improvement of lateral stability and safety.

### 4.3. Case 3. Single Lane and Double Lane Change Maneuvers

In this case, two kinds of steering inputs are given for testing handling performance, when the vehicle has over-steering behavior in cornering. Figures 24 and 25 show the results for the single lane-change maneuver. The yaw rate of both PS&ARS and AST & ARS can be very close to the ideal value, which indicates that the adjustment of vehicle attitude does not cause interference to ARS. On the other hand, it reflects that ARS has a greater weight in improving lateral stability. The important role of AST & ARS can be found in Figure 25. Compared with other systems, the global sideslip angle of ATS & ARS can be also reduced as much as possible. For a double lane change maneuver in Figures 26 and 27, the decreased trend of global sideslip angle still represent similar results as the previous cases. The collaborative system AST&ARS achieves better lateral stability and steering response in intense driving while ensuring the better heading directivity of the vehicle.

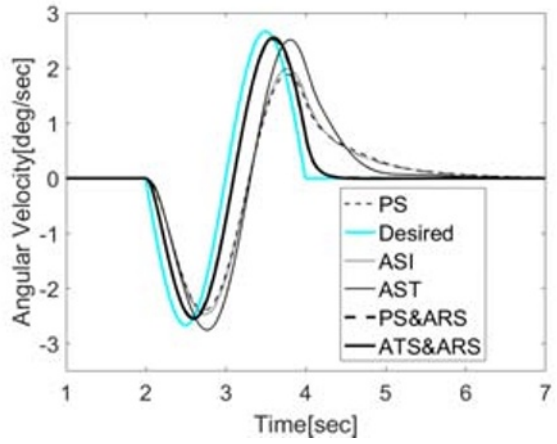


Figure 24. Yaw rate of vehicle with neutral steering behavior.

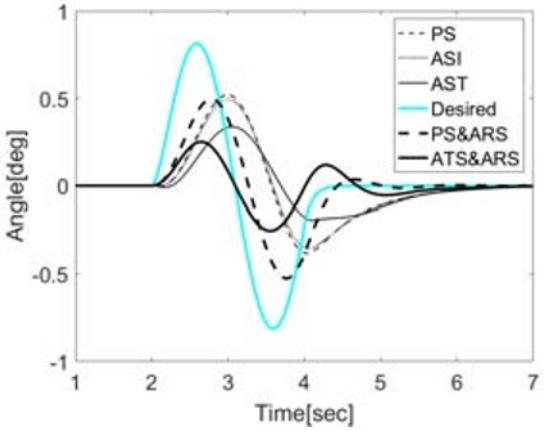


Figure 25. Global sideslip angle of the vehicle with over-steer behavior.

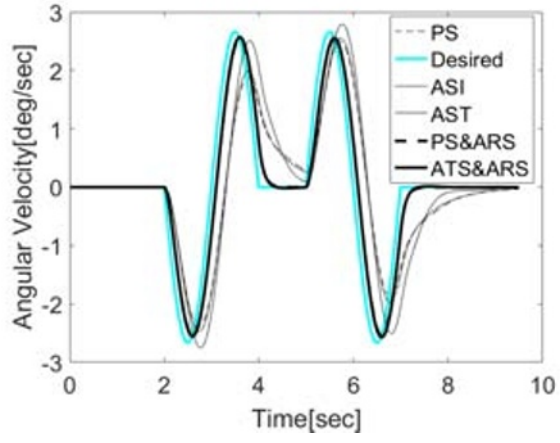


Figure 26. Yaw rate of vehicle with over-steering behavior.

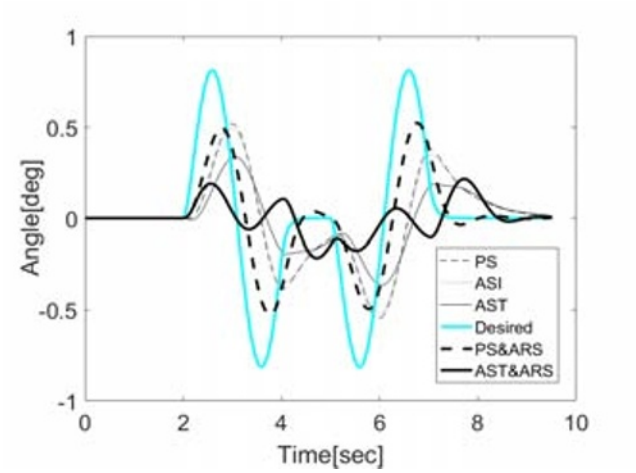


Figure 27. Global side slip angle of the vehicle with over-steer behavior.

## 5. CONCLUSION

By using the ability to evenly distribute the vertical dynamic load and the coupling effect of body angular motion and yaw motion, AST eliminates the adverse effect of centrifugal forces on ride comfort, moreover, plays a positive role in improving handling and safety performance of vehicles. ARS represents a strong ability for improving lateral stability and safety by keeping under neutral-steer behavior and reducing sideslip angle. In the analysis of various maneuvers, the ATS & ARS controller has no conflict in improving vehicle steering characteristics and further improves the lateral stability and safety of the vehicle. Finally, the cooperative control system mentioned in this paper realizes the synchronous improvement of vehicle ride comfort, handling, stability, and safety in cornering.

## REFERENCES

Ahmad, E., Iqbal, J., Arshad Khan, M., Liang, W. and Youn, I. (2020). Predictive control using active aerodynamic surfaces to improve ride quality of a vehicle. *Electronics* **9**, **9**, 1463.

Attia, T., Vamvoudakis, K. G., Kochersberger, K., Bird, J. and Furukawa, T. (2019). Simultaneous dynamic system estimation and optimal control of vehicle active suspension. *Vehicle System Dynamics* **57**, **10**, 1467–1493.

Cech, I. (2000). Anti-roll and active roll suspensions. *Vehicle System Dynamics* **33**, **2**, 91–106.

Čorić, M., Deur, J., Xu, L., Tseng, H. E. and Hrovat, D. (2018). Optimisation of active suspension control inputs for improved performance of active safety systems. *Vehicle System Dynamics* **56**, **1**, 1–26.

Esmailzadeh, E., Goodarzi, A. and Vossoughi, G. R. (2003). Optimal yaw moment control law for improved vehicle handling. *Mechatronics* **13**, **7**, 659–675.

Esmailzadeh, E., Vossoughi, G. R. and Goodarzi, A. (2001). Dynamic modeling and analysis of a four motorized wheels electric vehicle. *Vehicle System Dynamics* **35**, **3**, 163–194.

Farmer, C. M. (2004). Effect of electronic stability control on automobile crash risk. *Traffic Injury Prevention* **5**, **4**, 317–325.

Gáspár, P., Szabó, Z., Bokor, J. and Nemeth, B. (2016). Robust control design for active driver assistance systems. *Springer, DOI,* 10, 978-3.

Goodall, R. (1999). Tilting trains and beyond-the future for active railway suspensions. Part 1: Improving passenger comfort. *Computing & Control Engineering J.* **10**, **4**, 153–160.

Huashi, Z. J. W. S. L. (2008). Handling stability simulation and analysis of five-axle heavy-vehicle based on all-wheel steering [J]. *Trans. Chinese Society for Agricultural Machinery,* **9**.

Khan, H., Iqbal, J., Baizid, K. and Zielinska, T. (2015). Longitudinal and lateral slip control of autonomous wheeled mobile robot for trajectory tracking. *Frontiers of Information Technology & Electronic Engineering* **16**, **2**, 166–172.

Li, B., Rakheja, S. and Feng, Y. (2016). Enhancement of vehicle stability through integration of direct yaw moment and active rear steering. *Proc. Institution of Mechanical Engineers, Part D: J. Automobile Engineering* **230**, **6**, 830–840.

Li, F., Wang, L., Liao, C. and Wu, Y. (2014). Active steering control strategy of steer-by-wire system based on variable steering ratio. *2014 IEEE Conf. and Expo Transportation Electrification Asia-Pacific (ITEC Asia-pPacific)*, Beijing, China.

Liang, W., Khan, M. A., Youn, E., Youn, I. and Tomizuka, M. (2018). Attitude motion control of vehicle including the active passenger seat system. *Int. J. Vehicle Design* **78**, **1-4**, 131–160.

Lucet, E., Lenain, R. and Grand, C. (2015). Dynamic path tracking control of a vehicle on slippery terrain. *Control Engineering Practice,* **42**, 60–73.

Mirzaei, M. and Mirzaeinejad, H. (2012). Optimal design of a non-linear controller for anti-lock braking system. *Transportation Research Part C: Emerging Technologies,* **24**, 19–35.

Ni, L., Ma, F. and Wu, L. (2020). Posture control of a four-wheel-legged robot with a suspension system. *IEEE Access,* **8**, 152790–152804.

Saglam, F. and Unlusoy, Y. S. (2016). Adaptive ride comfort and attitude control of vehicles equipped with active hydro-pneumatic suspension. *Int. J. Vehicle Design* **71**, **1-4**, 31–51.

Scherbring, D. J. and Gust, J. R. (2013). All-wheel steering system and vehicle incorporating the same. U.S. Patent No. 8,528,685.

Smith, E. N., Velenis, E., Tavernini, D. and Cao, D. (2018). Effect of handling characteristics on minimum time cornering with torque vectoring. *Vehicle System Dynamics* **56**, **2**, 221–248.

Song, J. (2005). Performance evaluation of a hybrid electric brake system with a sliding mode controller. *Mechatronics* **15**, **3**, 339–358.

Tchamna, R., Youn, E. and Youn, I. (2014). Combined control effects of brake and active suspension control on the global safety of a full-car nonlinear model. *Vehicle System Dynamics* **52**, **supp.1**, 69–91.

Topalov, A. V., Oniz, Y., Kayacan, E. and Kaynak, O. (2011). Neuro-fuzzy control of antilock braking system using sliding mode incremental learning algorithm. *Neurocomputing* **74**, **11**, 1883–1893.

Wang, J. and Shen, S. (2008). Integrated vehicle ride and roll control via active suspensions. *Vehicle System Dynamics* **46**, **supp.1**, 495–508.

Wu, L., Youn, I. and Tomizuka, M. (2016). Integrated attitude motion and lateral stability control of a vehicle via active suspension and rear-wheel steering control system. *The Dynamics of Vehicles on Roads and Tracks: Proc. 24th Symp. Int. Association for Vehicle System Dynamics (IAVSD 2015),* Graz, Austria.

Youn, I., Im, J. and Tomizuka, M. (2006). Level and attitude control of the active suspension system with integral and derivative action. *Vehicle System Dynamics* **44**, **9**, 659–674.

Youn, I., Wu, L., Youn, E. and Tomizuka, M. (2015). Attitude motion control of the active suspension system with tracking controller. *Int. J. Automotive Technology* **16**, **4**, 593–601.

Zafeiropoulos, S. and Di Cairano, S. (2013). Vehicle yaw dynamics control by torque-based assist systems enforcing driver's steering feel constraints. *2013 American Control Conf.,* Washington, DC, USA.

Zhai, L., Sun, T. and Wang, J. (2016). Electronic stability control based on motor driving and braking torque distribution for a four in-wheel motor drive electric vehicle. *IEEE Trans. Vehicular Technology* **65**, **6**, 4726–4739.

Zhou, R., Zolotas, A. and Goodall, R. (2011). Integrated tilt with active lateral secondary suspension control for high speed railway vehicles. *Mechatronics* **21**, **6**, 1108–1122.

Zhou, R., Zolotas, A. and Goodall, R. (2014). Robust system state estimation for active suspension control in high-speed tilting trains. *Vehicle System Dynamics* **52**, **supp.1**, 355–369.